

Optical linear polarization of 74 white dwarfs with the RoboPol polarimeter

Michał Żejmo¹, Aga Słowikowska¹, Krzysztof Krzeszowski¹, Pablo Reig^{2,3},
and Dmitry Blinov^{2,3,4}

¹ Janusz Gil Institute of Astronomy, University of Zielona Góra, Lubuska 2, 65-265 Zielona Góra, Poland

² Foundation for Research and Technology, 71110 Heraklion, Crete, Greece

³ University of Crete, Physics Department, PO Box 2208, 710 03 Heraklion, Crete, Greece

⁴ Astronomical Institute, St. Petersburg State University, Universitetsky pr. 28, Petrodvoretz, 198504 St. Petersburg, Russia

Accepted XXX. Received YYY; in original form ZZZ

ABSTRACT

We present the first linear polarimetric survey of white dwarfs (WDs). Our sample consists of WDs of DA and DC spectral types in the SDSS *r* magnitude range from 13 to 17. We performed polarimetric observations with the RoboPol polarimeter attached to the 1.3-m telescope at the Skinakas Observatory. We have 74 WDs in our sample, of which almost all are low polarized WDs with polarization degree (PD) smaller than 1%, while only 2 have PD higher than 1%. There is an evidence that on average the isolated WDs of DC type have higher PD (with median PD of 0.78%) than the isolated DA type WDs (with median PD of 0.36%). On the other hand, the median PD of isolated DA type WDs is almost the same, i.e. 0.36% as the median PD of DA type white dwarfs in binary systems with red dwarfs (dM type), i.e. 0.33%. This shows, as expected, that there is no contribution to the PD from the companion if the WD companion is the red dwarf, which is the most common situation for WDs binary systems. We do not find differences in the polarization degree between magnetic and non-magnetic WDs. Because 97% of WDs in our sample have PD lower than 1%, they can be used as faint zero-polarized standard star in the magnitude range from 13 up to 17 of SDSS *r* filter. They cover the Northern sky between 13 hour to 23 hour in right ascension and from -11° to 78° in declination. Additionally, we found that for low extinction values (< 0.04) the best model that describes the dependence of PD on $E(B-V)$ is given by the equation: $PD_{\max, \text{ISM}}[\%] = 0.65 E(B-V)^{0.12}$.

Key words: standards – polarization – instrumentation: polarimeters – techniques: polarimetric – white dwarfs

1 INTRODUCTION

In the last years the interest in optical polarimetry has grown significantly (e.g. Marscher et al. 2010). The reason for this boom is that polarimetric measurements give an invaluable additional constrain on theoretical models that neither the photometry, astrometry nor spectrometry can provide. These studies include all kinds of astrophysical objects. There are regular monitoring campaigns to study the polarization changes of AGNs in the optical domain, as for example the optical monitoring of selected blazars with the RoboPol polarimeter (Pavlidou et al. 2014). There are also optical polarization studies of isolated neutron stars including pulsars (e.g. Słowikowska et al. 2009; Lundqvist et al. 2011; Moran et al. 2013, 2014; Mignani et al. 2015) and magnetars (e.g. Wang et al. 2015), as well as neutron stars in high

mass X-ray binaries (e.g. Reig et al. 2014, Słowikowska et al. in preparation) and low mass X-ray binaries (e.g. Baglio et al. 2014), not to mention polarization studies of GRBs (Mundell et al. 2013) and of polarized light from exoplanets for which a dedicated detector, i.e. Spectro-Polarimetric High-contrast Exoplanet REsearch (SPHERE) at VLT has been recently built¹.

The scientific community has started to use polarimetric measurements extensively to study stellar and non-stellar objects. However, reaching fainter objects by using infrastructure with larger mirror introduced a serious problem, namely, the lack of faint polarization standards of both types

¹ <https://www.eso.org/sci/facilities/paranal/instruments/sphere.html>

— the zero-polarized and polarized ones. Each measurement using a polarimeter or spectropolarimeter needs to be properly calibrated. Thus, the polarized standards are necessary to establish the intrinsic depolarization caused by the instrument, while the zero-polarized standards are necessary to get the instrumental polarization (e.g. the RINGO3 polarimeter at the Liverpool Telescope, see [Słowikowska et al. \(2016\)](#)).

The aim of our work is twofold: *i)* to perform a statistical analysis of the linear polarization properties of white dwarfs sample and *ii)* to provide observers with new faint linear polarimetric standard sources.

There are more than 23,000 WDs known up to date (see Sec. 2). For many of them their spectral type is known. Most of WDs atmospheres are hydrogen-rich atmospheres (DA), while almost all the rest are helium-rich (DB). However, a significant fraction of WDs also contain trace elements in their atmospheres and therefore they are labelled with Z for metals or Q for carbon, as for example DZ or DQ. There are also cases when the WD spectrum does not show any strong lines, but still their atmospheres are helium-rich. Such WDs are classified as DC type WDs. WDs with magnetic fields stronger than 1MG can be detected via Zeeman splitted lines, while weaker magnetic fields can be detected using spectropolarimetry. However, because DC type WDs spectra do not have strong spectral lines, therefore it is not possible to use the Zeeman effect to measure their magnetic field strength. Previous studies showed that around 10% up to 20% of all WDs are magnetised with strong magnetic field ([Ferrario et al. 2015](#), and references therein). The PD of magnetised WDs is between a fraction of a percent up to a few percent, as for example in case of GD 229 that has almost 8% of linear PD in R band ([Berdyugin & Piirola 1999](#)). The population of magnetised WDs can be even larger because the magnetic field of many sources is unknown.

Linear polarimetric population study can help to select WDs as good candidates for stable polarimetric calibration sources. Moreover, for each WD we have information about whether it is an isolated WD or WD in a binary system. In most cases the companion is a low mass red dwarf. Magnetised WDs in binary systems with low mass star that are in contact are classified as the magnetic cataclysmic variables (MCVs, i.e. polars and intermediate polars) and they represent one fourth of the whole CVs population ([Wickramasinghe & Ferrario 2000](#)). There are also binary systems composed of WD and low mass star that are close but are not in contact, i.e. pre-CVs, however none of such systems with magnetic WD is known so far ([Liebert et al. 2015](#)). There are close double degenerate systems and common proper motion binaries as well. This allows us to study the dependence of WD polarimetric properties on singularity or binarity, taking into account the type of the binary.

White dwarfs are commonly used as zero polarization standard stars. In the literature we can find eleven white dwarfs used for this purpose. Two of them, i.e. G191-B2B (PD=0.09%) and GD319 (PD=0.045%), were proposed by [Turnshek et al. \(1990\)](#) as the HST polarimetric standards, whereas another nine were proposed by [Fossati et al. \(2007\)](#) as main zero polarization standards for the FORS1 instrument on the VLT. The main goal of [Fossati et al. \(2007\)](#) was to find a group of faint polarized and non-polarized standard stars that can be used for calibration of big telescopes. His

sample consists of 30 stars of different types in the magnitude range from 6 to 14. However, WDs given by [Fossati et al. \(2007\)](#) are in the magnitude range from 11 to 13, with only one exception of 14 mag. In our work we propose to extend existing standard lists with additional 74 WDs as low linear polarization standards. The biggest advantage of WDs from our sample is that they are even fainter, i.e. in the SDSS *r* magnitude range from 13.2 (WD2149+021) up to 17 (WD2213+317), than those already available in the literature. In this way our sample is complementary to the earlier work. A larger group of zero polarization standards allows to find visible standard in convenient time of the night and position on the sky.

There were many polarization studies of large samples of white dwarfs conducted so far, for example: [Angel et al. \(1981\)](#); [Schmidt & Smith \(1995\)](#); [Putney \(1997\)](#); [Kawka et al. \(2007\)](#); [Jordan et al. \(2007\)](#); [Kawka & Vennes \(2012\)](#); [Landstreet et al. \(2015\)](#). Recently, [Bagnulo et al. \(2015\)](#) published a spectropolarimetric catalogue of 809 objects, obtained with the FORS/VLT instrument, that includes 70 WDs. However, there is only one WD common in both lists, ours and [Bagnulo et al. \(2015\)](#), i.e. WD2149+021. The crucial difference between above mentioned studies and our work is that our observations are the first WDs linear polarization survey, whereas the others measured the circular polarization.

We describe the selection method in Sec. 2, the observations in Sec. 3, while the data analysis in Sec. 4. Results and conclusions are given in Sec. 5 and Sec. 6, respectively.

2 SELECTED SAMPLE

Our sample was built up from the following catalogues: the White Dwarf Catalogue of Villanova University² ([McCook & Sion \(1999\)](#), hereafter VUWDC), "SDSS DR7 White Dwarf Catalog" ([Kleinman et al. \(2013\)](#), hereafter DR7WDC) and "Post-common envelope binaries from SDSS-XIV. The DR7 white dwarf-main-sequence binary catalogue" ([Rebassa-Mansergas et al. \(2012\)](#), hereafter DR7WDC-bin). We gathered 23,068 objects from those catalogues. However, it should be mentioned that there are 14,235, 18,913 and 2,248 WDs in the VUWDC, DR7WDC and DR7WDC-bin, respectively. Some of WDs are repeated in all three catalogues, therefore the final number of WDs, i.e. 23,068, is smaller than just a simple sum of WDs from these catalogues. Once the sky coordinates were extracted, we searched for their photometric brightness measurements in the following sky surveys: SDSS ([York et al. 2000](#); [Ahn et al. 2012](#)), UKIDSS ([Lawrence et al. \(2007\)](#), [Casali et al. \(2007\)](#), [Hewett et al. \(2006\)](#), [Hodgkin et al. \(2009\)](#), [Hambly et al. \(2008\)](#)), 2MASS ([Skrutskie et al. 2006](#)) and WISE ([Wright et al. 2010](#)). Of the 23,068 WDs, 18,877 have known spectral type. Based on the previously mentioned catalogues, the distribution of different types of WDs is as follows: DA - strong hydrogen lines 84.2%, DB - strong He I lines 8.2%, DC - no strong lines, continuous spectrum 4%, DO - strong He II lines 0.3%, DQ - strong carbon lines 1.6%, DZ - strong metal lines, excluding carbon 1.6%. The contribution of the binary systems in the

² <http://www.astronomy.villanova.edu/WDcatalog/>

WD population is on the level of 13%. However, this number can be higher in reality because the catalogues only indicate the confirmed binary systems.

Due to observational constraints, we selected objects brighter than 17 mag and visible from the 1.3-m telescope at the Skinakas Observatory³ in Greece during the time span when the observatory operates, i.e. from April to November. This selection resulted in 618 WDs of DA spectral type, 54 WDs of DB spectral type, 15 WDs of DC spectral type, and 70 with other or unknown spectral classification. There is no bias in the number of WDs in our Skinakas sample due to the fact that we only impose the brightness limit on SDSS $r < 17$ mag and apply visibility cuts. The sample is not biased with respect to binarity either as $\sim 20\%$ of the selected objects are confirmed binaries. We conclude that our sample is a complete unbiased sample of the whole population.

3 OBSERVATIONS

Our observations were performed at the Skinakas Observatory located in Crete, Greece. For our study we used the RoboPol⁴ polarimeter that is a linear polarimeter with two Wollaston prisms and two half-wave plates. It allows to measure the Stokes I, Q, U parameters simultaneously for all stellar objects within 13×13 arcmin² field of view and the scale of 0.435"/pixel (King et al. 2014). The measurements were performed with an aperture defined as $2.5 \times \text{FWHM}$, where FWHM is an average full width at half maximum of stellar images, which has a median value of 1.7 arcsec (4.0 pixels). All observations with the RoboPol are performed with the R Johnston filter. The exposure time was adjusted according to the brightness of each target, which was estimated during the short pointing exposures. It was calculated in such a way to ensure S/N ratio equal to 10 in the PD for a 2.5% polarized source. Moreover, 300 seconds overhead was needed for each target as operational time that includes slew time and positioning time.

We performed observations of 74 WDs between May 20th, 2014 and June 6th, 2014 with one single observation on October 24th, 2013, collecting a total observing time of around 14 hours. While performing the observations, we firstly concentrated on the DA and DC type WDs. Because the observations were cut short due to bad weather conditions, we were not able to observe any of the selected DB WDs. Each WDs was observed only once, but single observation consists of a few exposures with appropriate calculated exposure time. Later, all the images were aligned with subpixel accuracy and stacked together. The observing log is presented in Tab. 1, where the WD name, coordinates, binarity indication, spectral type, brightness and distance along with their corresponding errors, E(B-V), as well as the observation date are given. All r brightness values were obtained from the SDSS data base (Ahn et al. 2012). Their corresponding errors are not greater than 0.01 mag. At first, distances were taken from the spectroscopic measurements published by Holberg et al. (2008), because they also provided the errors. In other cases the most recent distance

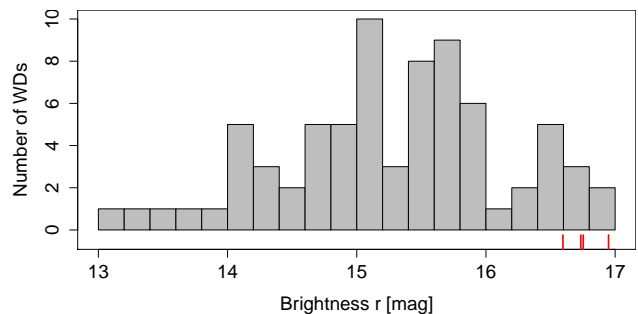


Figure 1. SDSS r brightness distribution of our WDs sample. The group consists of 74 WDs in total. Isolated DC type WDs are indicated with short red lines below the histogram.

measurements available in the literature were taken. We collected 51 distance measurements and 7 distance errors. All references for the spectral type and distance are provided in the table header. The values of E(B-V) were obtained from Schlafly & Finkbeiner (2011) using the NASA/IPAC Extragalactic Database (NED 2009).

There are 53 isolated WDs and 21 WDs in binary systems in our sample. Isolated WDs group consists of 49 DA WDs and 4 DC WDs (WD1402+649, WD1425+495, WD1524+566, WD1712+215), whereas the group of WDs in binary systems consists of 14 systems where the companion of the DA WD is the main sequence star, mainly red dwarf (11 DA+dM systems, as well as 2 DA+K7, and 1 DA+F8), and 7 double degenerated systems (DDSs) out of which 3 are classified as the DA+DA binaries, 2 are classified as DA+DC and the last 2 are WD+WD and WD+sdB. There are two magnetic WDs in our sample, i.e. WD1639+537 (GD 356) and WD1658+440 (PG 1658+440).

The RoboPol sensitivity is optimized for a source at the centre of the field by using a cross-shaped mask in the telescope focal plane. It reduces the sky background by a factor of 4 comparing the central target to the field stars. However, the mask also obscures part of the field, reducing the effective field of view. This plays the biggest role in case of one of our sources, i.e. WD1258+593 (PG1258+593, DA+DAH, $m_r = 15.5$). This source is a common proper motion binary system with the separation between components of 16 arc seconds (Girven et al. 2010) and its magnetic companion was behind the mask during the observations. Therefore, we were not able to measure its polarization.

The SDSS r brightness distribution of the observed WDs is shown in Fig. 1 with the mean of 15.3, whereas their distribution over the sky in the equatorial coordinates (α, δ) as well as in the galactic coordinates (l, b) are shown in the left and right panels of Fig. 2, respectively. There is a clear lack of WDs in our sample located in the Galactic latitude range between -20° and $+20^\circ$, i.e. in the location of the Galactic disk. It is caused by the fact, that surveys very often avoid this region of the sky.

³ <http://skinakas.physics.uoc.gr/en/>

⁴ <http://robopol.org/>

Table 1. RoboPol observation log of 74 white dwarfs: WD name, coordinates, binarity indication, where Y stands for WD in binary system and N for an isolated WD, WD spectral type, WD spectral type reference, brightness in SDSS *r* filter, distance with error and reference, E(B-V) and observation date. Spectral type references: B92 - Berg et al. (1992), F05 - Farihi et al. (2005), F97 - Ferrario et al. (1997), G10 - Girven et al. (2010), H12 - Holberg et al. (2012), K13 - Kleinman et al. (2013), K09 - Koester et al. (2009), L13- Limoges et al. (2013), M95 - Marsh et al. (1995), M99 - McCook & Sion (1999), M05 - Morales-Rueda et al. (2005), S10 - Schreiber et al. (2010), S05 - Silvestri et al. (2005). Distance references: G11 - Gianninas et al. (2011), H08 - Holberg et al. (2008), S14 - Sion et al. (2014). WDs common with Schmidt & Smith (1995) and Putney (1997) are marked with †.

WD Name	RA [hh:mm:ss]	Dec [dd:mm:ss]	Binary	Type	Type Ref.	<i>r</i> [mag]	Dist. [pc]	σ_{Dist} [pc]	Dist. Ref.	E(B-V)	Obs. Date
WD1257+037†	13:00:09.06	+03:28:41.0	N	DA	M99	15.6				0.02	2014-05-22
WD1258+593	13:00:35.19	+59:04:15.5	Y	DA+DAH	G10	15.5	65.0		G11	0.01	2014-05-22
WD1259+674	13:01:21.10	+67:13:07.3	N	DA	M99	16.4				0.01	2014-05-22
WD1310+583†	13:12:57.89	+58:05:11.2	N	DA	M99	14.2	21.1		S14	0.01	2014-06-05
WD1317+453†	13:19:13.71	+45:05:09.9	Y	WD+WD	M95	14.2	49.0		G11	0.03	2014-05-31
WD1319+466†	13:21:15.08	+46:23:23.7	N	DA	M99	14.7	36.0		G11	0.01	2014-06-05
WD1334+070	13:36:33.68	+06:46:26.8	Y	DA+DA	K09	15.5				0.03	2014-06-05
WD1344+106	13:47:24.36	+10:21:37.9	N	DA	M99	15.1	20.0	1.4	H08	0.03	2014-06-05
WD1344+572†	13:46:02.07	+57:00:32.7	N	DA	M99	13.6	20.0		S14	0.00	2014-05-31
WD1349+144	13:51:53.92	+14:09:45.4	Y	DA+DA	K09	15.4	85.0		G11	0.02	2014-06-05
WD1401+005	14:03:45.31	+00:21:36.0	N	DA	M99	15.0	463.0		G11	0.03	2014-06-05
WD1402+649	14:03:53.49	+64:39:53.7	N	DC	M99	16.9				0.01	2014-05-31
WD1407+374	14:09:23.26	+37:10:48.8	Y	DA+dM0	S10	14.8				0.01	2014-06-05
WD1407+425†	14:09:45.25	+42:16:00.8	N	DA	M99	15.1	31.0		G11	0.01	2014-05-31
WD1408+323†	14:10:26.95	+32:08:36.1	N	DA	M99	14.2	39.5	4.4	H08	0.01	2014-06-05
WD1415+132	14:17:40.25	+13:01:48.7	Y	DA+dM	K09	15.5	208.0		G11	0.02	2014-06-05
WD1420+518	14:22:41.92	+51:35:37.9	Y	DA+K7	K13	15.7				0.01	2014-06-05
WD1421+318	14:23:40.72	+31:34:59.8	N	DA	M99	15.6	112.0		G11	0.02	2014-06-05
WD1422+497	14:24:40.53	+49:29:58.1	Y	DA+K7	K13	15.7				0.02	2014-06-05
WD1425+495	14:26:59.41	+49:21:00.4	N	DC	M99	16.8				0.02	2014-05-31
WD1428+373	14:30:42.62	+37:10:15.4	Y	DA+DC	F05	15.6	97.0		G11	0.01	2014-06-05
WD1429+373	14:31:56.67	+37:06:30.0	N	DA	M99	15.5	123.0		G11	0.01	2014-05-31
WD1434+328	14:36:49.60	+32:37:34.5	Y	DA+dM0e	K13	15.9				0.01	2014-06-05
WD1440-025	14:43:35.06	-02:43:52.1	Y	DA+dMe	B92	15.7				0.06	2014-06-05
WD1446+286†	14:48:14.09	+28:25:11.8	N	DA	M99	14.8	48.0		G11	0.02	2014-06-05
WD1447+049	14:50:09.84	+04:41:45.7	N	DA	M99	15.6				0.04	2014-06-05
WD1449+168	14:52:11.40	+16:38:03.5	Y	DA+dM3	F05	15.6	102.0		G11	0.02	2014-06-05
WD1503-093	15:06:19.43	-09:30:20.8	N	DA	M99	15.3	57.0		G11	0.08	2014-06-05
WD1507-105	15:10:29.04	-10:45:19.4	N	DA	M99	15.4	51.0		G11	0.09	2014-06-05
WD1515+668	15:15:52.89	+66:42:42.8	N	DA	M99	15.5	32.0		G11	0.02	2014-05-31
WD1518-003	15:21:30.84	-00:30:55.7	N	DA	M99	15.5				0.06	2014-05-31
WD1524+566	15:25:42.95	+56:29:08.8	N	DC	M99	16.7				0.01	2014-05-31
WD1525+257	15:27:36.50	+25:35:06.0	N	DA	M99	15.9	87.0		G11	0.04	2014-06-05
WD1527+090	15:29:50.41	+08:55:46.4	N	DA	M99	14.5	53.0		G11	0.03	2014-05-31
WD1534+503	15:36:15.83	+50:13:51.1	N	DA	M99	15.8	38.0		G11	0.01	2014-06-01
WD1538+269	15:40:23.45	+26:48:29.8	Y	WD+sdB	M05	14.1				0.04	2014-05-20
WD1538+333	15:40:33.38	+33:08:52.5	N	DA	M99	15.1	22.7		S14	0.03	2014-06-01
WD1548+149	15:51:15.43	+14:46:59.2	N	DA	M99	15.3	83.0		G11	0.04	2014-06-01
WD1553+353†	15:55:02.10	+35:13:24.0	N	DA	M99	15.0				0.02	2014-05-31
WD1601+581†	16:02:41.70	+57:58:13.0	N	DA	M99	14.2	42.0		G11	0.02	2014-05-31
WD1606+422†	16:08:22.20	+42:05:43.2	N	DA	M99	14.0	45.0	7.1	H08	0.01	2014-05-31
WD1610+166	16:13:02.31	+16:31:55.5	N	DA	M99	15.9	65.4	18.4	H08	0.05	2014-06-01
WD1614+160	16:17:08.76	+15:54:38.5	N	DA	M99	15.7				0.03	2014-06-05
WD1630+089	16:32:33.18	+08:51:22.6	N	DA	M99	14.9	13.2		S14	0.05	2014-05-31
WD1631+396	16:33:39.31	+39:30:53.5	N	DA	M99	14.7	51.0		G11	0.01	2014-05-31
WD1632+177†	16:34:41.50	+17:36:32.0	N	DA	M99	13.4	15.0		G11	0.05	2014-05-31
WD1636+160	16:38:40.40	+15:54:17.0	N	DA	M99	15.8	68.0		G11	0.06	2014-06-05
WD1636+351	16:38:26.32	+35:00:11.9	N	DA	M99	15.1	111.0		G11	0.02	2014-05-31
WD1637+335†	16:39:27.82	+33:25:22.3	N	DA	M99	14.7	28.6	2.6	H08	0.02	2014-05-31
WD1639+537†	16:40:57.16	+53:41:09.6	N	DAP	F97	15.0	21.1		S14	0.02	2014-05-31
WD1641+387†	16:43:02.29	+38:41:17.3	N	DA	M99	14.8	43.0		G11	0.01	2014-05-31
WD1643+143	16:45:39.14	+14:17:46.2	Y	DA+dM	K09	15.1	133.0		G11	0.07	2014-05-31
WD1647+375†	16:49:20.29	+37:28:21.2	N	DA	M99	15.2	82.0		G11	0.02	2014-05-31
WD1654+637	16:54:29.01	+63:39:21.0	N	DA	M99	15.9	89.0		G11	0.02	2014-06-06
WD1655+215†	16:57:09.85	+21:26:50.2	N	DA	M99	14.4	23.3	1.7	H08	0.05	2014-05-31
WD1658+440†	16:59:48.41	+44:01:04.5	N	DAP	M99	15.0	22.0		S14	0.01	2014-05-31
WD1659+303†	17:01:08.02	+30:15:35.8	Y	DA+dM2	F05	15.1	50.0		G11	0.03	2014-05-31
WD1706+332	17:08:52.06	+33:12:58.5	Y	DA+F8	H12	16.1	81.0		G11	0.03	2014-05-31
WD1712+215	17:14:30.50	+21:27:11.3	N	DC	M99	16.6				0.05	2014-05-31
WD1713+695†	17:13:06.12	+69:31:25.7	N	DA	M99	13.5	27.0		G11	0.03	2014-05-31
WD1723+563	17:24:06.14	+56:20:03.1	Y	DA+dMe	K13	16.4				0.02	2014-06-01
WD1734+575	17:35:13.28	+57:30:12.2	N	DA	M99	16.7				0.05	2014-06-06
WD1738+669	17:38:02.53	+66:53:47.8	N	DA	M99	14.8	147.0		G11	0.04	2014-06-06
WD1827+778	18:25:09.28	+77:55:35.1	N	DA	M99	16.3	393.0		G11	0.07	2014-06-06
WD1833+644	18:33:29.21	+64:31:52.1	Y	DA+dM2e	K13	16.4	376.0		G11	0.04	2014-06-06
WD1842+412	18:44:12.63	+41:20:29.4	Y	DA+dM6e	K13	16.4				0.07	2014-06-01
WD2006+615	20:06:54.88	+61:43:10.4	N	DA	L13	16.3				0.14	2014-06-01
WD2058+083	21:01:13.37	+08:35:09.4	N	DA	M99	14.1	134.0		G11	0.07	2014-06-01
WD2126+734†	21:26:57.66	+73:38:44.5	Y	DA+DC	F05	14.3	21.2		S14	0.57	2014-06-06
WD2136+229	21:38:46.20	+23:09:21.5	N	DA	M99	15.2	38.0		G11	0.10	2014-06-06
WD2149+021†	21:52:25.38	+02:23:19.5	N	DA	M99	13.2	25.1	2.8	H08	0.06	2013-10-24
WD2213+317	22:15:06.96	+31:58:40.2	Y	DA+dM5	S05	17.0				0.08	2014-06-06
WD2236+313	22:38:22.74	+31:34:18.3	N	DA	M99	14.5				0.09	2014-06-06
WD2306+124	23:08:35.00	+12:45:40.2	N	DA	M99	15.3	63.0		G11	0.08	2014-06-06

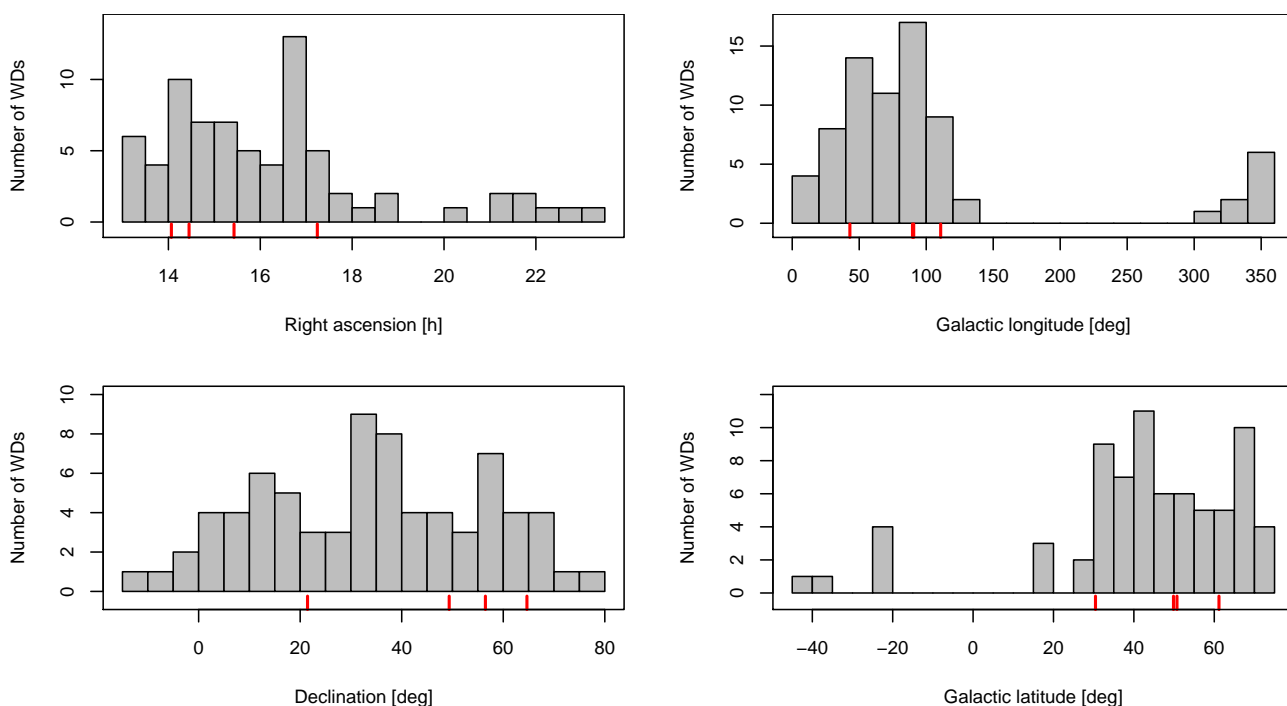


Figure 2. Distribution of WDs in the right ascension and the declination, as well as in the Galactic longitude and the Galactic latitude in the left and right columns, respectively. There is a clear lack of WDs in our sample located in the Galactic latitude range between -20° and $+20^\circ$, i.e. in the location of the Galactic disk. It is caused by the fact that surveys very often avoid this sky region. Isolated DC type WDs are indicated with short red lines below each histogram.

4 DATA ANALYSIS

The data were analysed with the standard RoboPol pipeline (King et al. 2014), whose output gives the normalised Stokes parameters $q = Q/I$ and $u = U/I$. Because most of our objects have very low polarization degree, it is important to account for any instrumental polarization. To this end, we obtained 22 measurements of the five zero-polarized standard stars given in Tab. 2. These measurements were performed during the time span of the WDs observations. The resulting values of q and u with their corresponding errors are shown in Fig. 3. Almost all of the points locate in the second quarter, indicating some residual instrumental polarization. To compute the instrumental polarization, we calculated the mean q and u values from 22 measurements of q and u of the zero-standard stars and obtained $\bar{u}_{inst} = -0.001$ and $\bar{q}_{inst} = 0.0033$, and thus the instrumental PD given by the equation

$$PD = \sqrt{q^2 + u^2} \quad (1)$$

equals to $0.34\% \pm 0.11\%$, where the error is the standard deviation (Tab. 3). The red cross in Fig. 3 marks the position of the averaged u and q parameters, while the lengths of its arms correspond to the respective standard deviation. The average values of \bar{u}_{inst} and \bar{q}_{inst} were then subtracted from the WDs measured u and q values. The results are given in Tab. 4 and are shown in Fig. 4. The standard deviations of \bar{u}_{inst} and \bar{q}_{inst} were propagated into the errors of the corrected WDs q and u values (corresponding σ_q and σ_u in Tab. 3). These values are also given in Tab. 4. The data corrected

for instrumental polarization were later used to obtain the PD according to Eq. 1, while the corresponding error (σ_{PD}) is calculated from Eq. 5 in King et al. (2014). Almost all the observed WDs have PD lower than 1%.

For low polarization signal-to-noise ratio ($PD / \sigma_{PD} < 3$) distribution of the PD is not normal (Gaussian). Additionally, the values of PD must always be positive so their uncertainties are not symmetric. This introduces a bias into any estimate. To deal with this problem we applied the debias method described by Vaillancourt (2006). First we checked the ratio between the PD and its error. In the case of PD/σ_{PD} lower than $\sqrt{2}$ the measured PD becomes 0.0 and only the upper sigma PD is given (most of our sources). In case of $\sqrt{2} < PD/\sigma_{PD} < 1.7$ the PD value and upper error are unchanged, while the lower error was changed so the lower limit of PD is equal to zero. We have three such cases in our sample, i.e. WD1440-025, WD1553+353 and WD1738+669. In case of $PD/\sigma_{PD} > 1.7$ the PD value is unchanged as well as the errors. Finally, in case of $PD/\sigma_{PD} > 3.0$ the PD value should be corrected according to the Eq. 12 of Vaillancourt (2006). However, we do not have any sources that fulfil the requirements of the last two mentioned cases. Obtained results as well as the corrected PD_c , $\sigma_{PD_c}^+$, $\sigma_{PD_c}^-$ are gathered in Tab. 4 in Sec. 5.

Table 2. Zero-polarized standard stars names, equatorial coordinates, as well as their brightness in USNO-A2.0 R filter and spectral types (ST). BD +28 4211 was classified as WD by [McCook & Sion \(1999\)](#), according to [Gianninas et al. \(2011\)](#) its type is sdO.

Name	RA	Dec	R	ST
HD 94851	10:56:44.25	−20:39:52.63	10.3	A5V
HD 154892	17:07:41.31	+15:12:37.61	7.9	F8V
BD +32 3739	20:12:02.15	+32:47:43.71	9.0	A0
BD +28 4211	21:51:11.02	+28:51:50.35	10.9	sdO
HD 212311	22:21:58.59	+56:31:52.75	8.5	A0

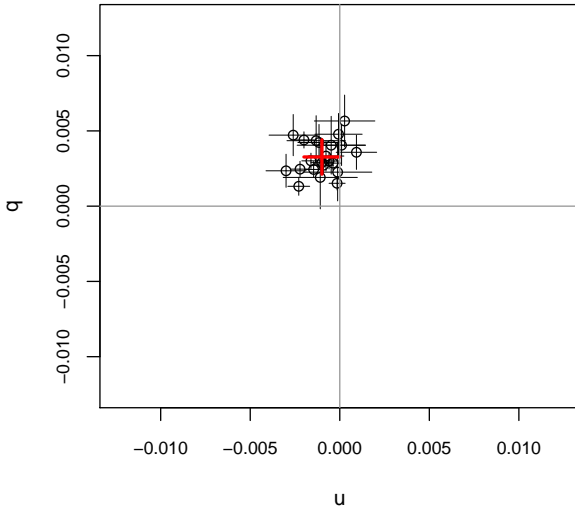


Figure 3. Diagram of q , u parameters of observed zero-polarized standard stars. The centre of the red cross corresponds to the mean values of q and u , while the lengths of its arms correspond to the respective standard deviation.

Table 3. Zero-polarized standard stars names, number of observations (NoO), the measured mean u and mean q values, together with the mean u and q values from all measurements. The PD calculated from the respective mean u and mean q is also given.

Name	NoO	\bar{u}	\bar{q}	PD [%]
HD 94851	2	-3×10^{-4}	0.0022	0.22
HD 154892	2	−0.0021	0.0029	0.36
BD +32 3739	5	−0.0011	0.0028	0.3
BD +28 4211	12	-8×10^{-4}	0.0038	0.39
HD 212311	1	−0.0022	0.0025	0.33
Mean value		−0.001	0.0033	0.34

5 RESULTS

5.1 Measured and corrected PD values

The results of our analysis, i.e. the data set with q and u Stokes parameters, measured PD as well as PD corrected for low ratio of PD / σ_{PD} values along with their corresponding errors are presented in Tab. 4.

Our results do not contain the q and u values of two well established zero-polarized standard white dwarfs, i.e. G 191-B2B and GD319. It is caused by the fact that G 191-B2B was not visible at that time from Crete, while GD319 was observed only once, but GD319 is a spectroscopic binary with the companion separation lower than 2-3 arcsec, therefore proper aperture photometry of this object is very difficult with the instrument such as RoboPol. However, in our other work on the calibration of the RINGO3 polarimeter, we showed that the G 191-B2B is a very stable and good zero-polarized standard (Słowikowska et al. 2016).

The distribution of measured PD regardless of WD spectral type or binarity is shown in Fig. 5. The plots of PD, σ_{PD} and PD / σ_{PD} with respect to SDSS r brightness are shown in Fig. 6. A correlation analysis between these parameters yields the following correlation coefficients: 0.48 (p-value = 1.665×10^{-5}), 0.66 (p-value = 1.287×10^{-10}) and 0 (p-value = 0.996), respectively. This suggests that there might be a dependence on the brightness in both cases of PD and σ_{PD} .

5.2 PD dependence on the interstellar extinction

Additionally, we checked correlations between polarimetric results and location (l , b) in the Galaxy, but we found none. However, the interstellar reddening $E(B-V)$ depends on the

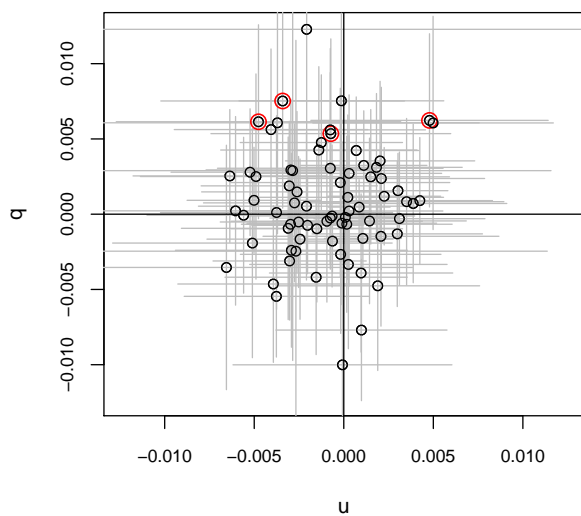


Figure 4. Diagram of q and u parameters of 74 observed WDs after correction for instrumental polarization. Red circles indicate isolated WDs of DC type. The ranges of the figure axes are the same as in Fig. 3 for easier comparison.

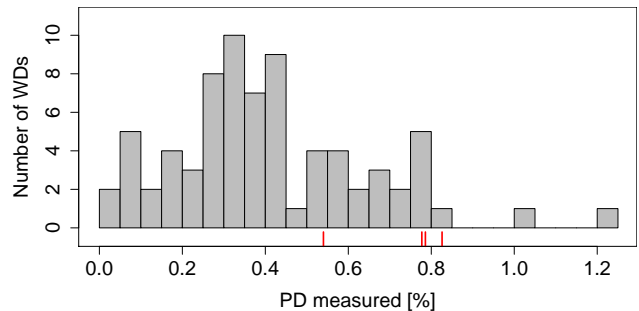


Figure 5. Distribution of measured PD regardless of the spectral type of WDs. Isolated DC type WDs are indicated with short red lines below the histogram.

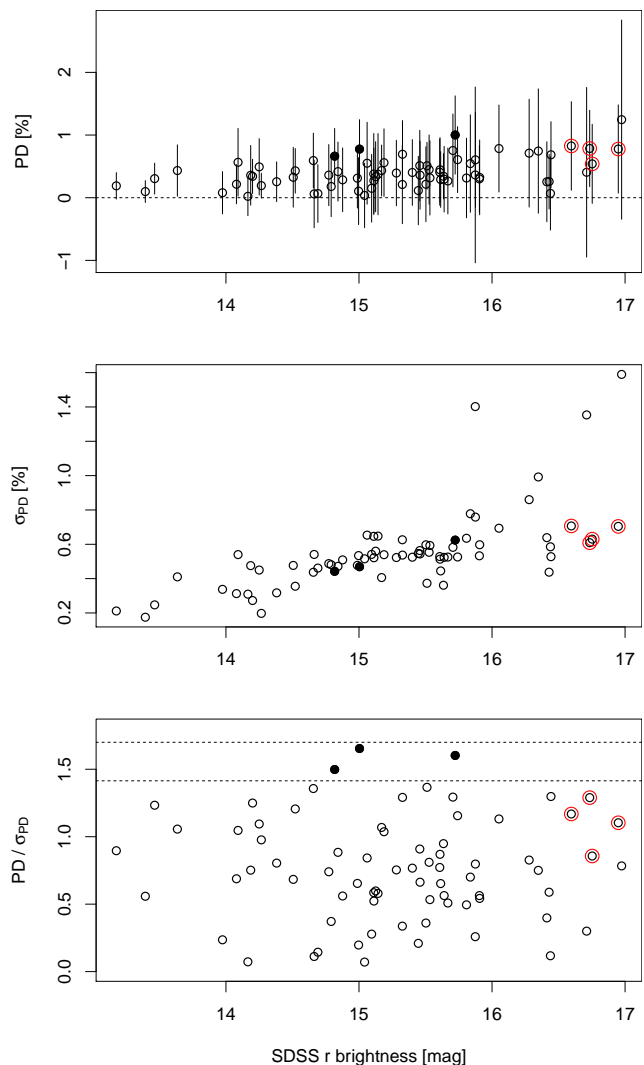


Figure 6. Calculated PD, σ_{PD} as well as the PD / σ_{PD} as a function of SDSS r brightness in the top, middle, and bottom panel, respectively. Black points denote measurements with PD / $\sigma_{PD} > \sqrt{2}$, while red circles indicate isolated DC type WDs. The horizontal lines in the bottom panel show $\sqrt{2}$ and 1.7 levels (see text for details as well as Tab. 4).

Table 4. Results of polarimetric observations of WDs with the RoboPol polarimeter: WD name, MJD of observation, normalised Stokes parameters q and u with instrumental polarization subtracted along with their respective errors, measured PD, σ_{PD} , corrected PD and its upper and lower errors (see text for details). WDs common with [Schmidt & Smith \(1995\)](#) and [Putney \(1997\)](#) are marked with † .

WD Name	MJD	q	σ_q	u	σ_u	PD	σ_{PD}	PD / σ_{PD}	PD _c	$\sigma_{PD_c}^+$	$\sigma_{PD_c}^-$
WD1257+037 †	56799.82	0.0032	0.0036	0.0011	0.0035	0.34	0.36	0.95	0.00	0.36	0.00
WD1258+593	56799.99	0.0009	0.0035	-0.0050	0.0037	0.51	0.37	1.37	0.00	0.37	0.00
WD1259+674	56799.87	-0.0005	0.0044	-0.0025	0.0044	0.26	0.44	0.59	0.00	0.44	0.00
WD1310+583 †	56813.79	0.0019	0.0043	-0.0030	0.0049	0.36	0.48	0.75	0.00	0.48	0.00
WD1317+453 †	56808.77	0.0048	0.0045	-0.0013	0.0045	0.49	0.45	1.09	0.00	0.45	0.00
WD1319+466 †	56813.80	0.0028	0.0042	-0.0052	0.0044	0.59	0.44	1.36	0.00	0.44	0.00
WD1334+070	56813.81	0.0024	0.0061	0.0021	0.0058	0.32	0.59	0.53	0.00	0.59	0.00
WD1344+106	56813.81	0.0025	0.0068	-0.0049	0.0065	0.55	0.65	0.84	0.00	0.65	0.00
WD1344+572 †	56808.78	-0.0031	0.0039	-0.0030	0.0043	0.43	0.41	1.06	0.00	0.41	0.00
WD1349+144	56813.82	-0.0039	0.0053	0.0010	0.0051	0.40	0.52	0.77	0.00	0.52	0.00
WD1401+005	56813.83	-0.0005	0.0054	-0.0009	0.0053	0.11	0.53	0.20	0.00	0.53	0.00
WD1402+649	56808.80	0.0061	0.0064	-0.0048	0.0079	0.78	0.70	1.10	0.00	0.70	0.00
WD1407+374	56813.83	0.0029	0.0047	-0.0030	0.0047	0.42	0.47	0.88	0.00	0.47	0.00
WD1407+425 †	56808.96	0.0001	0.0064	-0.0038	0.0065	0.38	0.65	0.58	0.00	0.65	0.00
WD1408+323 †	56813.84	-0.0002	0.0031	0.0001	0.0030	0.02	0.31	0.07	0.00	0.31	0.00
WD1415+132	56813.84	0.0008	0.0055	0.0035	0.0054	0.36	0.54	0.66	0.00	0.54	0.00
WD1420+518	56813.85	-0.0027	0.0053	-0.0002	0.0056	0.27	0.53	0.51	0.00	0.53	0.00
WD1421+318	56813.86	-0.0042	0.0051	-0.0015	0.0051	0.45	0.51	0.87	0.00	0.51	0.00
WD1422+497	56813.87	-0.0046	0.0052	-0.0039	0.0053	0.61	0.53	1.16	0.00	0.53	0.00
WD1425+495	56808.81	0.0054	0.0063	-0.0007	0.0067	0.54	0.63	0.86	0.00	0.63	0.00
WD1428+373	56813.88	0.0035	0.0053	0.0020	0.0053	0.41	0.53	0.77	0.00	0.53	0.00
WD1429+373	56808.98	-0.0048	0.0056	0.0019	0.0057	0.51	0.56	0.91	0.00	0.56	0.00
WD1434+328	56813.89	0.0015	0.0053	-0.0026	0.0053	0.30	0.53	0.56	0.00	0.53	0.00
WD1440-025	56813.90	-0.0100	0.0062	-0.0001	0.0061	1.00	0.62	1.60	1.00	0.62	1.00
WD1446+286 †	56813.90	-0.0010	0.0049	-0.0015	0.0048	0.18	0.48	0.37	0.00	0.48	0.00
WD1447+049	56813.92	0.0025	0.0045	0.0015	0.0044	0.29	0.44	0.65	0.00	0.44	0.00
WD1449+168	56813.93	-0.0017	0.0053	-0.0024	0.0052	0.30	0.52	0.56	0.00	0.52	0.00
WD1503-093	56813.93	0.0007	0.0053	0.0039	0.0052	0.39	0.52	0.75	0.00	0.52	0.00
WD1507-105	56813.94	0.0011	0.0055	0.0002	0.0053	0.11	0.55	0.21	0.00	0.55	0.00
WD1515+668	56808.99	0.0005	0.0049	-0.0021	0.0060	0.22	0.60	0.36	0.00	0.60	0.00
WD1518-003	56808.96	0.0043	0.0055	-0.0014	0.0055	0.45	0.55	0.81	0.00	0.55	0.00
WD1524+566	56808.83	0.0062	0.0058	0.0048	0.0066	0.79	0.61	1.29	0.00	0.61	0.00
WD1525+257	56813.96	-0.0009	0.0061	-0.0031	0.0060	0.32	0.60	0.54	0.00	0.60	0.00
WD1527+090	56808.89	0.0042	0.0036	0.0007	0.0035	0.43	0.36	1.21	0.00	0.36	0.00
WD1534+503	56809.00	-0.0019	0.0076	-0.0051	0.0078	0.55	0.78	0.70	0.00	0.78	0.00
WD1538+269	56798.00	-0.0007	0.0032	-0.0020	0.0031	0.22	0.31	0.69	0.00	0.31	0.00
WD1538+333	56809.01	-0.0024	0.0064	-0.0029	0.0065	0.38	0.65	0.58	0.00	0.65	0.00
WD1548+149	56809.01	0.0056	0.0054	-0.0041	0.0054	0.69	0.54	1.29	0.00	0.54	0.00
WD1553+353 †	56808.98	-0.0077	0.0047	0.0010	0.0048	0.78	0.47	1.65	0.78	0.47	0.78
WD1601+581 †	56808.84	0.0016	0.0025	0.0030	0.0028	0.34	0.27	1.25	0.00	0.27	0.00
WD1606+422 †	56808.90	-0.0003	0.0034	-0.0008	0.0034	0.08	0.34	0.24	0.00	0.34	0.00
WD1610+166	56809.02	-0.0025	0.0140	-0.0027	0.0140	0.36	1.40	0.26	0.00	1.40	0.00
WD1614+160	56813.99	0.0075	0.0058	-0.0001	0.0057	0.75	0.58	1.29	0.00	0.58	0.00
WD1630+089	56808.97	0.0008	0.0052	-0.0028	0.0051	0.29	0.51	0.56	0.00	0.51	0.00
WD1631+396	56808.90	-0.0006	0.0054	-0.0001	0.0053	0.06	0.54	0.11	0.00	0.54	0.00
WD1632+177 †	56808.89	0.0005	0.0018	0.0009	0.0017	0.10	0.18	0.56	0.00	0.18	0.00
WD1636+160	56813.99	0.0031	0.0064	-0.0008	0.0063	0.31	0.64	0.50	0.00	0.64	0.00
WD1636+351	56808.92	-0.0004	0.0055	0.0014	0.0054	0.15	0.54	0.28	0.00	0.54	0.00
WD1637+335 †	56808.91	-0.0001	0.0047	-0.0007	0.0046	0.07	0.46	0.14	0.00	0.46	0.00
WD1639+537 †	56808.85	-0.0003	0.0044	0.0031	0.0048	0.31	0.48	0.65	0.00	0.48	0.00
WD1641+387 †	56808.92	0.0031	0.0049	0.0018	0.0048	0.36	0.49	0.74	0.00	0.49	0.00
WD1643+143	56808.93	-0.0033	0.0056	0.0003	0.0055	0.33	0.56	0.60	0.00	0.56	0.00
WD1647+375 †	56808.95	-0.0001	0.0052	-0.0056	0.0054	0.56	0.54	1.04	0.00	0.54	0.00
WD1654+637	56814.01	0.0002	0.0063	-0.0060	0.0076	0.60	0.76	0.80	0.00	0.76	0.00
WD1655+215 †	56808.86	0.0012	0.0032	0.0023	0.0032	0.26	0.32	0.80	0.00	0.32	0.00
WD1658+440 †	56808.94	0.0002	0.0050	0.0003	0.0052	0.04	0.52	0.07	0.00	0.52	0.00
WD1659+303 †	56808.94	0.0027	0.0052	0.0003	0.0052	0.27	0.52	0.52	0.00	0.52	0.00
WD1706+332	56808.91	0.0061	0.0071	0.0050	0.0067	0.78	0.69	1.13	0.00	0.69	0.00
WD1712+215	56808.88	0.0075	0.0071	-0.0034	0.0068	0.83	0.71	1.17	0.00	0.71	0.00
WD1713+695 †	56808.95	-0.0007	0.0022	-0.0030	0.0025	0.30	0.25	1.23	0.00	0.25	0.00
WD1723+563	56809.04	-0.0015	0.0060	0.0021	0.0066	0.25	0.64	0.40	0.00	0.64	0.00
WD1734+575	56814.02	0.0029	0.0126	-0.0029	0.0144	0.41	1.35	0.30	0.00	1.35	0.00
WD1738+669	56814.03	-0.0055	0.0040	-0.0038	0.0051	0.66	0.44	1.50	0.66	0.44	0.66
WD1827+778	56814.04	0.0061	0.0074	-0.0037	0.0113	0.71	0.86	0.83	0.00	0.86	0.00
WD1833+644	56814.05	0.0025	0.0044	-0.0064	0.0054	0.69	0.53	1.30	0.00	0.53	0.00
WD1842+412	56809.07	-0.0007	0.0059	0.0002	0.0059	0.07	0.59	0.12	0.00	0.59	0.00
WD2006+615	56809.07	-0.0035	0.0081	-0.0066	0.0104	0.74	0.99	0.75	0.00	0.99	0.00
WD2058+083	56809.08	0.0056	0.0054	-0.0008	0.0053	0.57	0.54	1.05	0.00	0.54	0.00
WD2126+734 †	56814.06	-0.0016	0.0019	0.0011	0.0021	0.19	0.20	0.98	0.00	0.20	0.00
WD2136+229	56814.07	0.0009	0.0042	0.0042	0.0041	0.43	0.41	1.07	0.00	0.41	0.00
WD2149+021 †	56589.88	-0.0018	0.0021	-0.0006	0.0021	0.19	0.21	0.90	0.00	0.21	0.00
WD2213+317	56814.08	0.0123	0.0159	-0.0021	0.0154	1.25	1.59	0.78	0.00	1.59	0.00
WD2236+313	56814.09	-0.0013	0.0048	0.0030	0.0048	0.33	0.48	0.68	0.00	0.48	0.00
WD2306+124	56814.09	0.0021	0.0063	-0.0002	0.0061	0.21	0.63	0.34	0.00	0.63	0.00

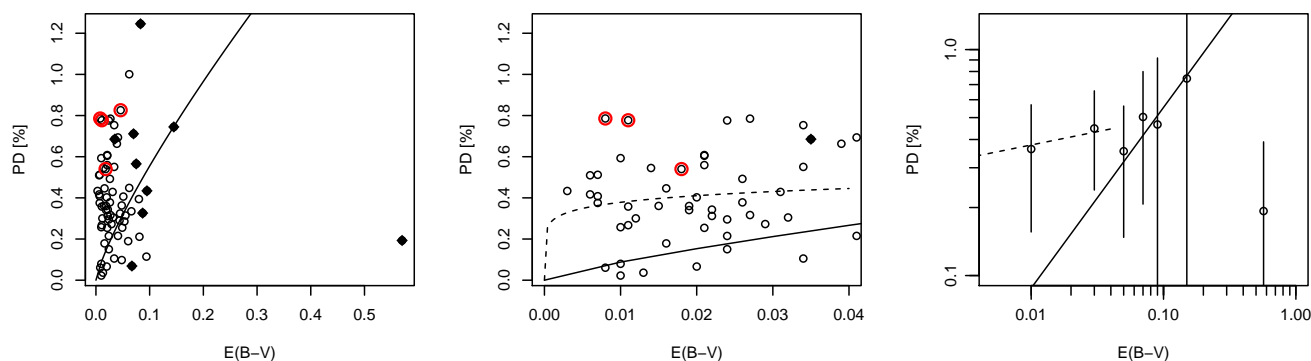


Figure 7. Dependence of the PD on the interstellar extinction for observed WDs. Values of $E(B-V)$ were obtained from [Schlafly & Finkbeiner \(2011\)](#) using the NASA/IPAC Extragalactic Database ([NED 2009](#)). The left and middle panels differ only with the x-axis range, while the right panel (log-log) shows data averaged in extinction bins of size 0.02. The red circles indicate isolated DC type WDs, while the black rhombuses indicate the WDs with the Galactic latitude between -30° and $+30^\circ$. The solid lines show expected dependence of the PD on $E(B-V)$ given by Eq. (2). The dashed lines show the dependence of the PD on $E(B-V)$ for the extinction range between 0.0–0.04 with the Eq. (3). Object WD2126+734 with the highest $E(B-V) = 0.57$ has PD equal to 0.19%. The error bars are omitted for clarity in the left and middle panels. In the right panel the errors are taken as standard deviations of measurements that fall into particular bin, apart for the last two bins. In those bins only single measurements were available and their individual σ_{PD} were taken as the errors.

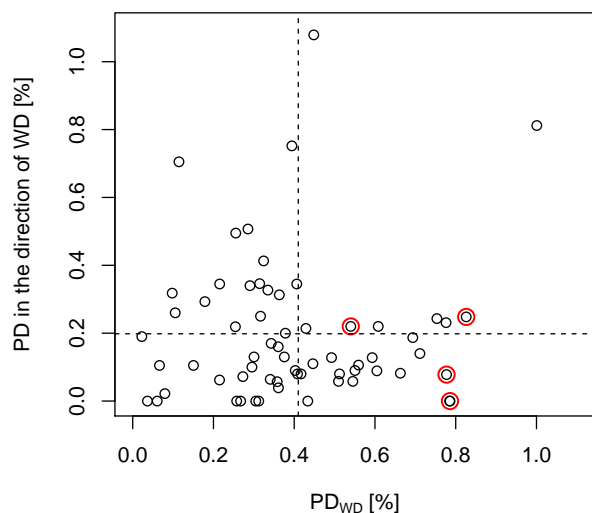


Figure 8. Measured PD values from [Berdyugin et al. \(2014\)](#) in the direction of a given WD within the 3° radius vs. WDs measured PD. Isolated DC type WDs are marked with red circles. WD1440–025 that has $PD \sim 1\%$, is classified as DA+dMe. Dashed lines denote respective mean PD values. The error bars are omitted for clarity.

location of the source in the Galaxy. Therefore, we also studied the PD–extinction relationship as described by [Fosalba et al. \(2002\)](#) who found it to be of the form of

$$PD_{\max, \text{ISM}}[\%] = 3.5 E(B-V)^{0.8}. \quad (2)$$

Fig. 7 shows the PD as a function of $E(B-V)$ for all WDs in our sample. The relation described by the Eq. (2) is shown in the figure with the black solid lines. Our data range from 0.003 to 0.57 in terms of reddening, because most of the stars are closer than 500 pc. They also have small PD ($<1\%$). [Fosalba et al. \(2002\)](#) $E(B-V)$ binned data range from 0.1 to 1.0, with one exception of $E(B-V) = 0.05$, as it is shown in their log-log scale Fig. 4. For comparison, we also binned our data in extinction with the bin size of 0.02. Resulting plot is shown in the right panel of Fig. 7, where we have 7 points that are averages of 26, 22, 12, 7, 5, 1, 1 measurements, respectively. Most of the points are located in the lower $E(B-V)$ -bins. The sixth and seventh bins correspond to WD2006+615 and WD2126+734 with $E(B-V)$ values of 0.145 and 0.57 and PD of 0.74% and 0.19%, respectively. PD errors in the right panel of Fig. 7 are taken as standard deviations of measurements that fell into particular bin but for the last two bins individual σ_{PD} were taken. It can be seen that the first two values (first and second bin) significantly diverge from model (Eq. 2, shown as black solid line in all panels of Fig. 7). It is worth noticing that most of extinction values of our WDs, 48 out of 74 measurements, fall into the first two bins with $E(B-V)$ below 0.04. Therefore, we fitted the $a \cdot E(B-V)^b$ model to that data and got the following relation in the extinction range from 0.0 up to 0.04:

$$PD_{\max, \text{ISM}}[\%] = 0.65 E(B-V)^{0.12} \quad (3)$$

This dependence is plotted as dashed line in the middle and right panels of Fig. 7.

5.3 Comparison of our measurements with the PD survey

We also compared the measured PD of WDs in our sample with the catalogue values of PD obtained by [Berdyugin](#)

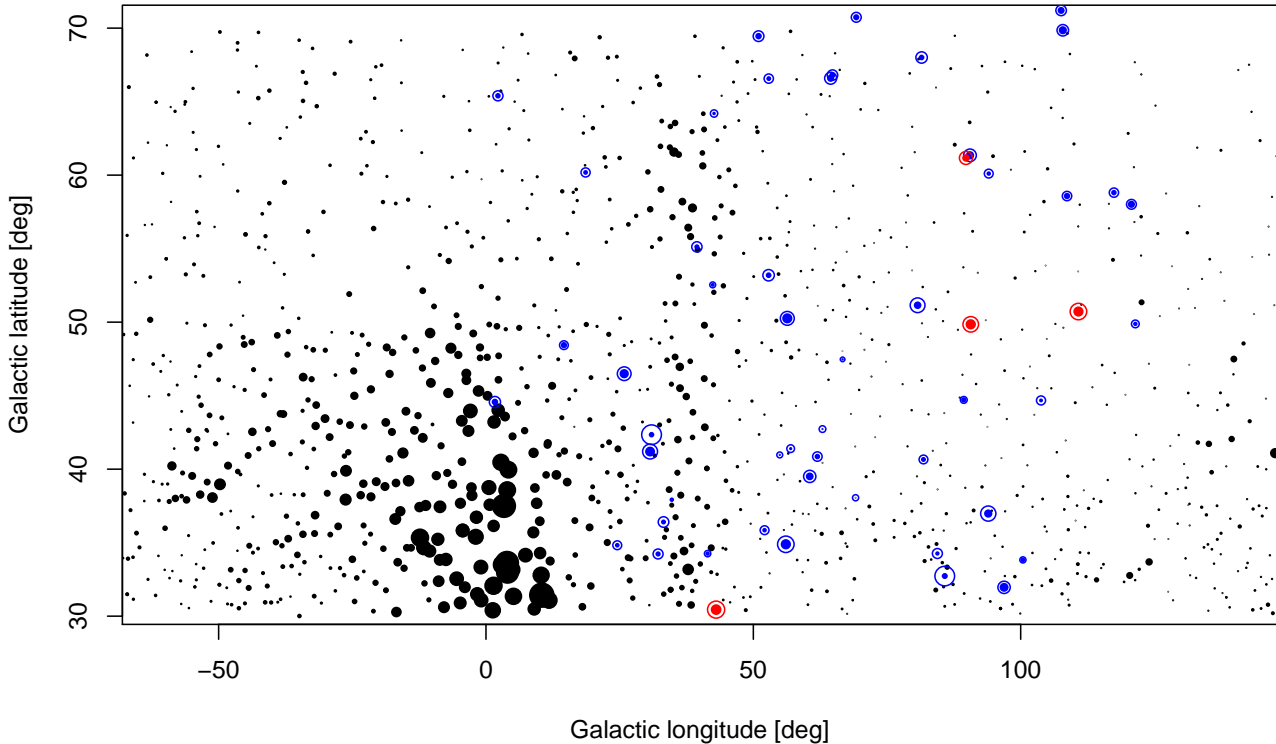


Figure 9. The spatial distribution of our WDs sample in galactic coordinates in comparison to Berdyugin et al. (2014) measurements. Size of the filled black circles corresponds to the PD value measured by Berdyugin et al. (2014), whereas the diameter of colour circles corresponds to the PD value measured by us, red circles indicate the isolated DC WDs, whereas the blue circles indicate all other WDs. Open circles denote upper limit of measured PD, i.e. $PD + \sigma_{PD}$. As can be seen, there are regions in the Galaxy that show higher polarization degree, however DC WDs from our sample are not located in these regions, therefore their PD most likely is not influenced by the background polarization.

et al. (2014), who collected PD measurements of ~ 3600 stars within the distance of 600 pc. To get galactic polarization maps they took the data in the V band. They excluded variable and peculiar stars which might possess intrinsic polarization. More than 60% of stars in their sample show polarization below 0.5%. Only around 200 stars have PD higher than 0.5%, up to values exceeding 1%. We have the distance value for 51 WDs in our sample, where the closest one is 13.2 pc away and the farthest has a distance of 463 pc (Tab. 1). For each WD in our sample we searched for neighbouring stars in the VizieR Online Data Catalog "Polarization at high galactic latitude" (Berdyugin et al. 2014) within the radius of 3° . We found 64 cases that allowed us to compare our WD measurements with catalogue PD values what is shown in Fig. 8. We can see that an average PD from the Berdyugin et al. (2014) measurements in the direction to WDs from our sample is on the level of $0.2\% \pm 0.03\%$, whereas the mean PD of these 64 WDs is $0.4\% \pm 0.03\%$. The sample distributions are not similar (the two sample Student's t-Test gives $p\text{-value} = 3.819 \times 10^{-7}$), therefore at least part of the measured PD of WDs from our sample is intrinsic. This seems to be confirmed by the spatial distribution of our WDs sam-

ple in galactic coordinates in comparison to Berdyugin et al. (2014) measurements that is shown in Fig. 9. There are regions in the Galaxy that show higher polarization degree, however for example DC WDs from our sample are not located in these regions. Still, higher PD of DC WDs might be biased by the fact that we are close to the telescope limits in terms of brightness.

5.4 Spectral type and binarity comparison

The comparison of PD distributions of both types of isolated WDs in the form of a boxplot is presented in Fig. 10. It can be seen that DC type white dwarfs on average have higher PD than DA type WDs. However, the sample sizes are unequal with the ratio of 10:1 in the favour of DA type WDs. For a validation a bootstrap experiment was conducted. We drew 10000 samples of size 4 from DA type WDs with replacement and recorded median PD value. In less than 0.01% of all cases (1 out of 10000) the median value of PD from DA type WDs was greater than that of DC. The median of all median PD values agrees with that of the whole isolated DA sample.

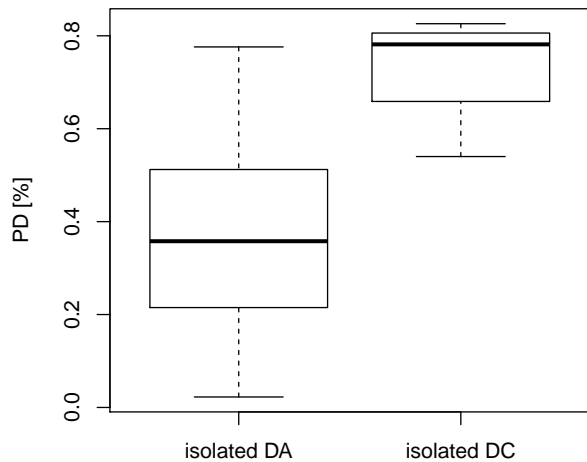


Figure 10. Comparison of PD of isolated DA and isolated DC type white dwarfs in form of a box plot. The thick black line inside the rectangle denotes the median value of the sample. The rectangle covers 50% of the points lying between 1st and 3rd quartiles. The upper and the lower whiskers denote either extremal value from the dataset (maximum or minimum, respectively) lying in the 1.5 IQR (interquartile range) distance from the rectangle or 1.5 IQR itself, whichever is closer. These two groups are clearly different. The DC type WDs show higher PD. One should be aware that there are only 4 isolated white dwarfs of DC spectral type in the sample.

In our sample we have 21 binary systems. In Fig. 11 we compare isolated DA WDs (49) with DA+dM binaries (11) and double degenerated systems (DDs, 7) with respect to their PD. The samples show similar properties with comparable median PD values. Three bootstrap experiments were conducted similarly to the previous case and they confirmed the results presented in Fig. 11. This suggests, as expected, that there is no significant contribution to the PD from the companion that in most cases of WDs binary systems is a red dwarf. There are two DA+dM outliers in Fig. 11, i.e. WD1440+025 and WD2213+317. WD1440+025 is classified as a DA+dMe binary, while WD2213+317 is located close to the Galactic disc ($b \simeq -20^\circ$), has high proper motion (Ivanov 2008), and at the same time, it is the faintest object in our WD sample.

5.5 Magnetic WDs and WDs with measured magnetic field

Magnetic fields of isolated magnetic WDs (MWDs) are in the range between $10^3 - 10^9$ G, with quite well established upper limit, but rather uncertain lower limit (Ferrario et al. 2015). The magnetic field of white dwarfs in magnetic cataclysmic variables (MCVs) varies between 7–230 MG (Ferrario et al. 2015). A comparison of our target list with the surveys by Schmidt & Smith (1995) and Putney (1997) reveals that there are two highly MWDs and 20 WDs with measurable

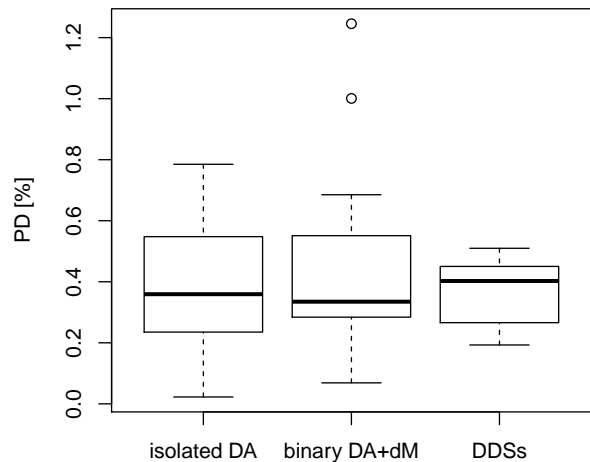


Figure 11. Comparison of PD of isolated DA type white dwarfs, DA+dM binaries and double degenerate systems (DDs) presented as a box plot similar as in Fig. 10. Outliers, i.e. WD1440+025 and WD2213+317, lying outside the whiskers range are plotted individually.

but rather low (with respect to MWDs) or not significant magnetic field values ($B \sim$ kG) in our sample. These 22 objects are marked with a † in Tab. 4.

The two known isolated, highly MWDs ($B > 1$ MG) in our sample are WD1639+537 (GD 356) and WD1658+440 (PG 1658+440). Both have the same DA spectral type and have similar SDSS r brightness of around 15 mag. Thus taking into account only isolated WDs (53 out of 74), only 3.8% of our sample are highly MWDs. WD1639+537 not only has a high surface magnetic field of the order of 11.2 ± 1.1 MG (Greenstein & McCarthy 1985), but it is also photometrically variable. Its variability is most likely caused by the dark spot that covers 10% of the stellar surface (Brinkworth et al. 2004). WD1658+440 has a mean surface magnetic field on the level of 2.3 ± 0.5 MG (Liebert et al. 1983), confirmed later by Schmidt et al. (1992) to be 2.3 ± 0.2 MG. The maximum circular spectropolarimetric values of WD1639+537 and WD1658+440 are $\pm 2.3\%$ (from Fig. 1. of Ferrario et al. 2015) and 4.8% (Tab. 2 of Liebert et al. 1983, also later confirmed by Schmidt et al. 1992, see Fig. 1 of their work with the circular polarization spectra, where maximum V values reach around $\pm 5\text{--}6\%$ in $H\alpha$ and $H\beta$ lines). Whereas their linear PD (this work) is on the level of $0.31\% \pm 0.48\%$ and $0.04\% \pm 0.52\%$, respectively. However, in both cases the corrected linear PD is zero with the upper error on the level of $\sim 0.5\%$. The reason for such a low linear polarization must be the same as that for the low value of circular continuum polarization ($V=0.01 \pm 0.047\%$, Angel et al. 1981), namely, the dilution over the broad band range of the Johnson R filter.

The fact that we have only $\sim 4\%$ of isolated MWDs in our sample is roughly consistent with results presented in the

magnitude limited surveys. As stated by Schmidt & Smith (1995), the incidence of magnetism among WDs is found to be $4.0\% \pm 1.5\%$ for fields between $\sim 3 \times 10^4$ and 10^9 G. Similarly, Kepler et al. (2013) found by detectable Zeeman splittings that around 4% of all observed DAs have magnetic fields in the range from 1 to 733 MG.

On the other hand, there are 20 WDs in our sample for which the magnetic field measurements were performed resulting with magnetic fields below 1 MG ($\text{kG} < B < \text{MG}$). 19 out of these 20 WDs are described by Schmidt & Smith (1995) and one by Putney (1997). We should note here that there is one more WD in Putney (1997) common with our list, but with no magnetic field value (see later in the paragraph for details). From Schmidt & Smith (1995) they are as follow, isolated: WD1310+583, WD1319+466, WD1344+572, WD1407+425, WD1408+323, WD1446+286, WD1553+353, WD1601+581, WD1606+422, WD1632+177, WD1637+335, WD1641+387, WD1647+375, WD1655+215, WD1713+695, WD2149+021 and in binary systems: WD1317+453, WD1659+303 and WD2126+734. The highest measured absolute value of the magnetic field strength in this group is on the level of 13.8 kG (WD1317+453), but one should notice that in many cases the measurement is affected by large uncertainty. We can also compare our results with the circular spectropolarimetric survey of Putney (1997, hereafter P97). Out of 52 WDs that she measured only two of them are in our sample, i.e. WD1257+037 (G60–54, $m_r = 15.6$) and WD1712+215 (G170–27, $m_r = 16.6$). The first one is of the DA type (DAQZ8 in P97), while the second is the DC type (DC7 in P97). Only in the first case the author was able to calculate the magnetic field based on the circularly polarized absorption lines and she obtained $B_e = 11.2 \pm 18.0$ kG. In case of WD1712+215 the magnetic field strength could not be estimated because it does not show absorption features nor circular polarization. P97 suggested an upper limit of 20 MG. Our results of linear PD for both WDs are $0.34\% \pm 0.36\%$ and $0.83\% \pm 0.71\%$, respectively. However, both corrected linear PD are zero with the upper error on the level of 0.36% and 0.71% for WD1257+037 and WD1712+215, respectively. While the circular polarization values are $V_{\text{red}}[\%] = +0.045 \pm 0.073$, $V_{\text{blue}}[\%] = +0.092 \pm 0.156$ and $V_{\text{red}}[\%] = +0.088 \pm 0.038$, $V_{\text{blue}}[\%] = +0.008 \pm 0.066$ for WD1257+037 and WD1712+215, respectively (see Putney 1997 for details).

Apparently, even in case of two highly MWDs with the magnetic field on the order of a few MG we do not detect significant linear polarization degree. This is likely caused by the fact of the polarization dilution over broad band. Therefore, we conclude that the MWDs (at least those of our sample) can also be used as zero-polarimetric standards.

6 SUMMARY AND CONCLUSIONS

We conclude that most of the measured WDs, being of DA and DC spectral types and in the SDSS r magnitude range from 13 to 17, have low PD below 1%. Only WD1440–025 and WD2213+317 have PD higher than 1%. We found out that there is a correlation between the measured PD and r brightness, as well as between the σ_{PD} and r brightness.

Moreover, the DC type white dwarfs on average have higher PD (with the median PD of 0.78%) than DA type WDs (with the median PD of 0.36%). The significance of the difference (p-value of the null hypothesis) is on the level of 0.01. Taking into account that the PD and PD uncertainties show the dependence on the brightness the difference between those two WD types can be attributed to the fact that the DC type WDs are fainter than DA. However, there are only 4 DC type WDs in our sample, so we can not state this without any doubts. On the other hand, there seems to be no difference between PD of isolated DA type WDs (0.36%) and binary systems that include DA type WDs (0.35%).

Our sample constitutes a set of good candidates of faint linear polarimetric standard stars with SDSS r magnitudes ranging from 13 up to 17. They are well distributed in the right ascension range from 13 hour up to 24 hour mostly on the Northern sky with declination from -11° up to 78° . Moreover, we enrich the present low linear polarization WDs standard list by a factor of five. Reaching fainter objects with infrastructure with larger mirror introduced a serious problem, namely, the lack of faint polarization standards of both types, the zero-polarized and polarized ones. The presented list of WDs addresses this need with respect to zero-polarized standard stars and is complementary to the previous work done by Fossati et al. (2007), which includes nine WDs in the magnitude range from 11 to 13, with only one exception of 14 mag.

Additionally, we found that for low extinction values (< 0.04) the best model that describes the dependence of PD on $E(B-V)$ is given by the equation: $\text{PD}_{\text{max,ISM}}[\%] = 0.65 E(B-V)^{0.12}$.

Even in cases of highly MWDs, as well as in the cases of low magnetic field WDs, we do not detect significant linear polarization degree. This is likely caused by the fact of the polarization dilution over broad band. Therefore, we conclude that even the MWDs of our sample can be very well used as polarimetric standards.

It will be very useful to perform deeper and longer observations on the DC type WDs to obtain measurements with higher accuracy and to expand the test sample. It is worth mentioning that Gaia satellite will discover around 100,000 WDs. Assuming the same ratio of around 300/23,000 (WDs brighter than 17 mag visible from the Skinakas Observatory to the total number of known WDs), there will be around 1,300 Gaia WDs brighter than 17 mag visible at Skinakas, therefore we will be able to continue our study in the future on much bigger sample.

ACKNOWLEDGEMENTS

This work has been supported by Polish National Science Centre grant DEC-2011/03/D/ST9/00656 (AS, KK, MŻ). This research was partly supported by the EU COST Action MP1104 "Polarization as a tool to study the solar system and beyond" within STSM projects: COST-STSM-MP1104-14064, COST-STSM-MP1104-16823 COST-STSM-MP1104-14070 and COST-STSM-MP1104-16821. DB acknowledges support from the St. Petersburg Univ. research grant 6.38.335.2015. RoboPol is a collaboration involving the University of Crete, the Foundation for Research and Technology - Hellas, the California Institute of Technology,

the Max-Planck Institute for Radioastronomy, the Nicolaus Copernicus University, and the Inter-University Centre for Astronomy and Astrophysics. This work was partially supported by the "RoboPol" project, which is co-funded by the European Social Fund (ESF) and Greek National Resources, and by the European Commission Seventh Framework Programme (FP7) through grants PCIG10-GA-2011-304001 "JetPop" and PIRSES-GA-2012-31578 "EuroCal". Data analysis and figures were partly prepared using R (R Core Team 2013).

REFERENCES

- Ahn C. P., et al., 2012, *ApJS*, **203**, 21
- Angel J. R. P., Borra E. F., Landstreet J. D., 1981, *ApJS*, **45**, 457
- Baglio M. C., Mainetti D., D'Avanzo P., Campana S., Covino S., Russell D. M., Shahbaz T., 2014, *A&A*, **572**, A99
- Bagnulo S., Fossati L., Landstreet J. D., Izzo C., 2015, *A&A*, **583**, A115
- Berdugugin A. V., Piirola V., 1999, *A&A*, **352**, 619
- Berdugugin A., Piirola V., Teerikorpi P., 2014, *A&A*, **561**, A24
- Berg C., Wegner G., Foltz C. B., Chaffee Jr. F. H., Hewett P. C., 1992, *ApJS*, **78**, 409
- Brinkworth C. S., Burleigh M. R., Wynn G. A., Marsh T. R., 2004, *MNRAS*, **348**, L33
- Casali M., et al., 2007, *A&A*, **467**, 777
- Farihi J., Becklin E. E., Zuckerman B., 2005, *ApJS*, **161**, 394
- Ferrario L., Wickramasinghe D. T., Liebert J., Schmidt G. D., Biegging J. H., 1997, *MNRAS*, **289**, 105
- Ferrario L., de Martino D., Gänsicke B. T., 2015, *Space Sci. Rev.*, **191**, 111
- Fosalba P., Lazarian A., Prunet S., Tauber J. A., 2002, *ApJ*, **564**, 762
- Fossati L., Bagnulo S., Mason E., Landi Degl'Innocenti E., 2007, in Sterken C., ed., *Astronomical Society of the Pacific Conference Series Vol. 364, The Future of Photometric, Spectrophotometric and Polarimetric Standardization*. p. 503
- Gianninas A., Bergeron P., Ruiz M. T., 2011, *ApJ*, **743**, 138
- Girven J., Gänsicke B. T., Külebi B., Steeghs D., Jordan S., Marsh T. R., Koester D., 2010, *MNRAS*, **404**, 159
- Greenstein J. L., McCarthy J. K., 1985, *ApJ*, **289**, 732
- Hambly N. C., et al., 2008, *MNRAS*, **384**, 637
- Hewett P. C., Warren S. J., Leggett S. K., Hodgkin S. T., 2006, *MNRAS*, **367**, 454
- Hodgkin S. T., Irwin M. J., Hewett P. C., Warren S. J., 2009, *MNRAS*, **394**, 675
- Holberg J. B., Bergeron P., Gianninas A., 2008, *AJ*, **135**, 1239
- Holberg J. B., Oswalt T. D., Barstow M. A., 2012, *AJ*, **143**, 68
- Ivanov G. A., 2008, *Kinematika i Fizika Nebesnykh Tel*, **24**, 480
- Jordan S., Aznar Cuadrado R., Napiwotzki R., Schmid H. M., Solanki S. K., 2007, *A&A*, **462**, 1097
- Kawka A., Vennes S., 2012, *MNRAS*, **425**, 1394
- Kawka A., Vennes S., Schmidt G. D., Wickramasinghe D. T., Koch R., 2007, *ApJ*, **654**, 499
- Kepler S. O., et al., 2013, *MNRAS*, **429**, 2934
- King O. G., Blinov D., Ramaprakash A. N., Myserlis I., et al. A., 2014, *MNRAS*, **442**, 1706
- Kleinman S. J., et al., 2013, *ApJS*, **204**, 5
- Koester D., Voss B., Napiwotzki R., Christlieb N., Homeier D., Lisker T., Reimers D., Heber U., 2009, *A&A*, **505**, 441
- Landstreet J. D., Bagnulo S., Valyavin G. G., Gadelshin D., Martin A. J., Galazutdinov G., Semenko E., 2015, *A&A*, **580**, A120
- Lawrence A., et al., 2007, *MNRAS*, **379**, 1599
- Liebert J., Schmidt G. D., Green R. F., Stockman H. S., McGraw J. T., 1983, *ApJ*, **264**, 262
- Liebert J., Ferrario L., Wickramasinghe D. T., Smith P. S., 2015, *ApJ*, **804**, 93
- Limoges M.-M., Lépine S., Bergeron P., 2013, *AJ*, **145**, 136
- Lundqvist N., Lundqvist P., Björnsson C.-I., Olofsson G., Pires S., Shibanov Y. A., Zyuzin D. A., 2011, *MNRAS*, **413**, 611
- Marscher A. P., Jorstad S. G., Larionov V. M., Aller M. F., Aller H. D., et al. 2010, *ApJ*, **710**, L126
- Marsh T. R., Dhillon V. S., Duck S. R., 1995, *MNRAS*, **275**, 828
- McCook G. P., Sion E. M., 1999, *ApJS*, **121**, 1
- Mignani R. P., Moran P., Shearer A., Testa V., Słowikowska A., Rudak B., Krzeszowski K., Kanbach G., 2015, *A&A*, **583**, A105
- Morales-Rueda L., Marsh T. R., Maxted P. F. L., Nelemans G., Karl C., Napiwotzki R., Moran C. K. J., 2005, *MNRAS*, **359**, 648
- Moran P., Shearer A., Mignani R. P., Słowikowska A., De Luca A., Gouïffès C., Laurent P., 2013, *MNRAS*, **433**, 2564
- Moran P., Mignani R. P., Shearer A., 2014, *MNRAS*, **445**, 835
- Mundell C. G., et al., 2013, *Nature*, **504**, 119
- NED 2009, The NASA/IPAC Extragalactic Database. California Institute of Technology, Pasadena, USA, <https://ned.ipac.caltech.edu>
- Pavlidou V., Angelakis E., Myserlis I., Blinov D., King O. G., et al. 2014, *MNRAS*, **442**, 1693
- Putney A., 1997, *ApJS*, **112**, 527
- R Core Team 2013, R: A Language and Environment for Statistical Computing. R Foundation for Statistical Computing, Vienna, Austria, <http://www.R-project.org>
- Rebassa-Mansergas A., Nebot Gómez-Morán A., Schreiber M. R., Gänsicke B. T., Schwöpe A., Gallardo J., Koester D., 2012, *MNRAS*, **419**, 806
- Reig P., Blinov D., Papadakis I., Kylafis N., Tassis K., 2014, *MNRAS*, **445**, 4235
- Schlaflly E. F., Finkbeiner D. P., 2011, *ApJ*, **737**, 103
- Schmidt G. D., Smith P. S., 1995, *ApJ*, **448**, 305
- Schmidt G. D., Bergeron P., Liebert J., Saffer R. A., 1992, *ApJ*, **394**, 603
- Schreiber M. R., et al., 2010, *VizieR Online Data Catalog*, **351**
- Silvestri N. M., Hawley S. L., Oswalt T. D., 2005, *AJ*, **129**, 2428
- Sion E. M., Holberg J. B., Oswalt T. D., McCook G. P., Wasatonic R., Myszkowski J., 2014, *AJ*, **147**, 129
- Skrutskie M. F., et al., 2006, *AJ*, **131**, 1163
- Słowikowska A., Kanbach G., Kramer M., Stefanescu A., 2009, *MNRAS*, **397**, 103
- Słowikowska A., Krzeszowski K., Żejmo M., Reig P., Steele I., 2016, *MNRAS*, **458**, 759
- Turnshek D. A., Bohlín R. C., Williamson II R. L., Lupie O. L., Koornneef J., Morgan D. H., 1990, *AJ*, **99**, 1243
- Vaillancourt J. E., 2006, *PASP*, **118**, 1340
- Wang Z., Tanaka Y. T., Wang C., Kawabata K. S., Fukazawa Y., Itoh R., Tziamtzis A., 2015, *ApJ*, **814**, 89
- Wickramasinghe D. T., Ferrario L., 2000, *PASP*, **112**, 873
- Wright E. L., et al., 2010, *AJ*, **140**, 1868
- York D. G., Adelman J., Anderson Jr. J. E., Anderson S. F., Annis J., Bahcall N. A., Bakken J. A., 2000, *AJ*, **120**, 1579